A Renewal Weakest-Link Model of Strength Distribution of Polycrystalline Silicon MEMS Structures

Zhifeng Xu
Department of Civil, Environmental, and Geo- Engineering,
University of Minnesota,
500 Pillsbury Dr. S.E.,
Minneapolis, MN 55455
e-mail: xuxx0877@umn.edu

Roberto Ballarini
Department of Civil and Environmental Engineering,
University of Houston,
N127, Engineering Building 1,
4726 Calhoun Road,
Houston, TX 77204
e-mail: rballari@Central.UH.EDU

Jia-Liang Le[1]
Department of Civil, Environmental, and Geo- Engineering,
University of Minnesota,
500 Pillsbury Dr. S.E.,
Minneapolis, MN 55455
e-mail: jle@umn.edu

Experimental data have made it abundantly clear that the strength of polycrystalline silicon (poly-Si) microelectromechanical systems (MEMS) structures exhibits significant variability, which arises from the random distribution of the size and shape of sidewall defects created by the manufacturing process. Test data also indicated that the strength statistics of MEMS structures depends strongly on the structure size. Understanding the size effect on the strength distribution is of paramount importance if experimental data obtained using specimens of one size are to be used with confidence to predict the strength statistics of MEMS devices of other sizes. In this paper, we present a renewal weakest-link statistical model for the failure strength of poly-Si MEMS structures. The model takes into account the detailed statistical information of randomly distributed sidewall defects, including their geometry and spacing, in addition to the local random material strength. The large-size asymptotic behavior of the model is derived based on the stability postulate. Through the comparison with the measured strength distributions of MEMS specimens of different sizes, we show that the model is capable of capturing the size dependence of strength distribution. Based on the properties of simulated random stress field and random number of sidewall defects, a simplified method is developed for efficient computation of strength distribution of MEMS structures. [DOI: 10.1115/1.4043440]

Keywords: renewal theory, size effect, strength statistics, structural reliability, weakest-link model

1 Introduction

Microelectromechanical Systems (MEMS) have found use in numerous technologies, including transportation systems, energy conversion, biochemical threat detection, medical devices, etc. [1,2]. It has been shown that the strength of polycrystalline silicon (poly-Si), the work horse of MEMS devices, exhibits considerable variability [3,4]. Meanwhile, it is generally accepted that the design of MEMS devices should target a failure risk of the order of 10^{-4} or lower. Therefore, understanding and modeling the probability distribution of failure strength of poly-Si MEMS structures have become an important subject especially for devices that operate under conditions of high stress and large deformation [2].

Over the past two decades, there has been a continuing interest in studying the strength statistics of MEMS structures [2,5–8]. Fabrication procedures inevitably lead to poly-Si structures whose sidewalls are characterized by a highly random geometry containing stress-concentrating and in-turn failure initiating sharp corners [5,9]. The random sidewall geometry obviously implies the uncertainty in the degree of stress concentration. Meanwhile, the local material strength may also exhibit some spatial variability. The combination of random sidewall geometry and material strength gives rise to the uncertainties in both the failure location and the overall strength of MEMS structures.

The biggest challenge in the modeling of failure statistics of MEMS structures is the aforementioned requirement of low failure risk [5]. Although direct experimental testing and brute-force stochastic simulations can provide useful statistical information such as the sample mean and standard deviation, they could not practically probe the left tail of the strength distribution that is required for high reliability design. Therefore, analytical modeling becomes an indispensable means for studying the strength distribution of MEMS structures.

The most widely used analytical model for strength distribution is the infinite weakest-link model, in which the structure is represented, from the statistical viewpoint, by a chain comprised of an infinite number of material elements [10,11]. By further assuming that the failure strengths of the elements are statistically independent, one can show that the probability distribution of structural strength belongs to the class of extreme value statistics [11–13]. Extensive experimental data on brittle structures have indicated that, among the three extreme distribution functions, the Weibull distribution is the only valid option. However, it has been consistently observed that the Weibull distribution is unable to provide optimum fitting of the measured strength distributions of MEMS specimens [7,8,14–16]. As an empirical remedy, the three-parameter Weibull distribution was proposed to improve the fitting [9,17]. However, it was determined that the model parameters strongly depend on the specimen size, a result that cannot be physically justified, and thus limits the prediction capability of the three-parameter Weibull model. Recent studies have also shown that the three-parameter Weibull distribution could lead to an overestimation of design strength for large-size structures [16,18–20].

The inapplicability of the Weibull distribution is rooted in the fact that the sizes of many poly-Si MEMS structures and/or their components (beams in resonators for example) are not sufficiently large as compared to the characteristic dimension of the material, e.g. grain size and sidewall defect size. Consequently, the structure cannot be represented by an infinite chain model. To address this issue, a finite weakest-link model was developed for poly-Si MEMS structures [16]. In the model, the sidewall defects were

[1]Corresponding author.

Contributed by the Applied Mechanics Division of ASME for publication in the Journal of Applied Mechanics. Manuscript received February 20, 2019; final manuscript received April 8, 2019; published online May 17, 2019. Assoc. Editor: Yonggang Huang.

modeled as V-notches of random depth and angle [8]. The structure was statistically represented by a finite chain of elements, where each element contains a single V-notch. The failure probability of each element was calculated by considering both the random geometry of V-notch and random material strength. It was shown that this model is able to provide optimum fits of the measured strength distributions of specimens of different sizes by using the same set of model parameters. However, the model considers equal spacing between the defects along the sidewall, which is certainly an oversimplification.

In a recent study, a first-passage based probabilistic model was proposed for failure of MEMS structures [21]. The model was formulated by directly using the continuous random fields of material strength and applied stress. The spatial autocorrelation features of these random fields were also explicitly included in the model. The failure probability was calculated through a level excursion analysis. Although this model provides a more physical representation of the probabilistic failure along the sidewalls, the computational cost is much higher as compared to the finite weakest-link model. In addition, some detailed statistical information, such as the autocorrelation functions of the random strength field, is not easily accessible.

The aforementioned finite weakest-link model is easy to use but with some oversimplifications. On the other hand, the first-passage model provides more physical insights into the failure statistics at a significant amount of computational cost. In this study, we develop a probabilistic model for the strength of poly-Si MEMS structures by combining the finite weakest-link model and the renewal theory. The model removes the key oversimplification used in the previous finite weakest-link model, while retaining the desirable computational efficiency of the weakest-link model.

2 Model Formulation

We limit our attention to uniaxial tension specimens since they are the most commonly used configurations for measuring the strength of the poly-Si used to fabricate MEMS devices. For the purposes of stress analysis, the sidewall grooves created by the fabrication procedures are modeled as V-notches. Based on the experimental observations [9], it is reasonable to consider that the specimen attains its peak load capacity once a catastrophic crack initiates at one of the notches. Note that this consideration may not hold for other loading scenarios, for example a system of parallel cracks (a limiting case of V-notches) under thermal stresses or fluid pressure [22–24]. The location of fracture initiation along the sidewall of the MEMS device is intrinsically random since the sidewall V-notches have random geometries and the local material resistance is also assumed to vary spatially.

Consider a specimen of length L subjected to remote stress σ_N (Fig. 1(*a*)). Each sidewall of the specimen contains some number of segments whose length is a random variable (Fig. 1(*b*)).

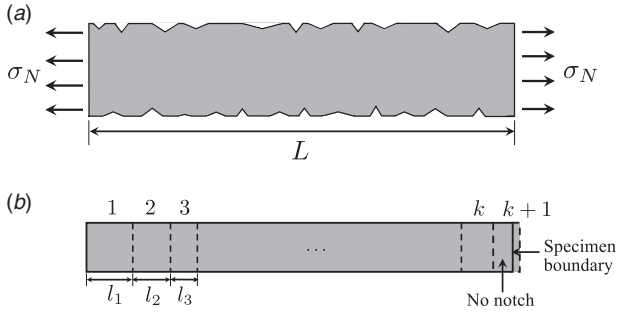

Fig. 1 (*a*) Uniaxial tensile MEMS specimen with sidewall defects idealized by V-notches and (*b*) schematic of the renewal weakest-link model for failure of a sidewall

Except for the last segment, a V-notch exists in the middle of each segment. Based on the foregoing discussion, we consider that only segments with V-notches would contribute to the failure of the specimen. Let k be the number of V-notches along each sidewall. Clearly, for a given specimen length L, the number k is intrinsically random. The survival probability, or reliability, of the specimen under stress σ_N can be calculated as

$$R_s(\sigma_N, L) = \left[\sum_{k=1}^{\infty} R(\sigma_N, L, k)\right]^2 \tag{1}$$

where $R(\sigma_N, L, k)$ = survival probability of a sidewall of length L that contains k number of V-notches. The failure probability, or equivalently the probability distribution of structural strength, of the specimen is simply $P_f(\sigma_N, L) = 1 - R_s(\sigma_N, L)$.

If the sidewall of length L consists of k number of V-notches, we must have

$$\sum_{i=1}^{k} l_i \le L \quad \text{and} \quad \sum_{i=1}^{k+1} l_i > L \tag{2}$$

where l_i = length of ith segment. The total length of $k+1$ segments would be larger than the actual sidewall length L (Fig. 1(*b*)). However, this is inconsequential since what matters for the failure statistics of the specimen is the first k number of segments with V-notches, whose total length is no greater than L.

Let $f(x)$ be the probability density function (pdf) of the segment length. The overall reliability of the first segment is given by $\int_0^L f(l_1)R_e(\sigma_N, l_1)\mathrm{d}l_1$, where $R_e(\sigma_N, l)$ = reliability of the segment of length l. The length of the second segment must satisfy $0 \le l_2 \le L - l_1$, and therefore the overall reliability of the second one is given by $\int_0^{L-l_1} f(l_2)R_e(\sigma_N, l_2)\mathrm{d}l_2$. Following the same analysis, the overall reliability of the kth segment is given by $\int_0^{L-l_1\cdots-l_{k-1}} f(l_k)R_e(\sigma_N, l_k)\mathrm{d}l_k$. The aforementioned consideration only enforces the condition $\sum_{i=1}^{k} l_i \le L$. To further satisfy $\sum_{i=1}^{k+1} l_i > L$, we also require $l_{k+1} \ge L - l_1 \cdots - l_k$.

As mentioned previously, the survival of each sidewall requires that all segments survive. By assuming the failure of the segments are statistically independent from each other, we have

$$R(\sigma_N, L, k) = \int_0^L \int_0^{L-l_1} \cdots \int_0^{L-l_1-l_2\cdots-l_{k-1}} \left[\prod_{i=1}^{k} f(l_i)R_e(\sigma_N, l_i)\right] \times F_c(L - l_1 - l_2 \cdots - l_k)\mathrm{d}l_k\mathrm{d}l_{k-1}\cdots\mathrm{d}l_1 \tag{3}$$

where $F_c(x) = \int_x^{\infty} f(y)\mathrm{d}y$ = complementary cumulative distribution function (cdf) of the segment length. The integral in Eq. (3) can be calculated in a recursive manner by noting that

$$R(\sigma_N, x, k) = \int_0^x S_e(\sigma_N, l)R(\sigma_N, x - l, k - 1)\mathrm{d}l \tag{4}$$

$$\text{and} \quad R(\sigma_N, x, 1) = \int_0^x S_e(\sigma_N, l)F_c(x - l)\mathrm{d}l \tag{5}$$

where $S_e(\sigma_N, l) = f(l)R_e(\sigma_N, l)$.

The reliability function $R_e(\sigma_N, l)$ of each segment is calculated based on the probabilistic failure of the V-notch. Consider a segment of MEMS containing a V-notch under tensile stress σ_N (Fig. 2). The fracture of V-notch has been extensively studied, and both strength and energy-based failure criteria have been proposed [25–30]. Since the focus of this study is on uniaxial tension specimens, for which the primary failure mode is mode I fracture, we adopt a simple nonlocal strength criterion. We consider that the crack starts to propagate from the V-notch tip once the nonlocal

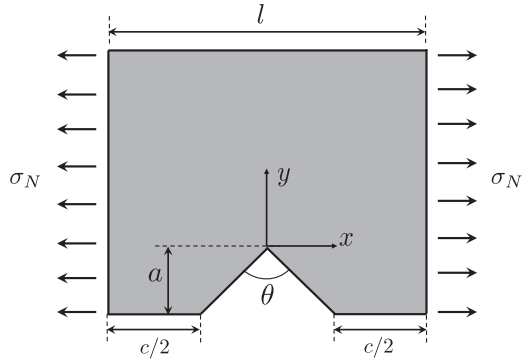

Fig. 2 Analysis of a notched segment

stress σ evaluated at the notch tip reaches the material tensile strength, i.e.

$$\sigma = r_c^{-1}\int_0^{r_c}\sigma_{xx}(y)\mathrm{d}y = f_t \tag{6}$$

where r_c is an averaging length scale, σ_{xx} = tensile stress in x-direction, and f_t = tensile strength of the material. The choice of nonlocal stress in the present failure criterion takes into account the finite fracture process zone (FPZ) formed at the notch tip, whose size is proportional to the length scale r_c.

Since the nonlocal stress is calculated from elastic analysis, we may rewrite the failure criterion (Eq. (6)) as

$$\sigma_N z(a, \theta, l) = f_t \tag{7}$$

where z is a dimensionless stress, which depends on the notch depth a, notch angle θ, and segment length l. Clearly z is a random variable, which is independent of the random material strength f_t. Therefore, the reliability of a segment of length l can be written as

$$R_e(\sigma_N, l) = \Pr\left(f_t/z \geq \sigma_N | l\right) = 1 - \int_0^{\infty} F_{f_t}(x\sigma_N) f_z(x|l)\mathrm{d}x \tag{8}$$

where $F_{f_t}(x)$ is the cdf of material strength, $f_z(x|l)$ is the conditional pdf of the dimensionless stress for given segment length l. This conditional pdf can be calculated as

$$f_z(x|l) = f_{zl}(x, l)/f(l) \tag{9}$$

where $f_{zl}(x, l)$ is the joint pdf of dimensionless stress and segment length, which needs to be evaluated numerically. Based on Eqs. (8) and (9), we can rewrite the term $S_e(\sigma_N, l)$ in Eq. (4) as

$$S_e(\sigma_N, l) = f(l) - \int_0^{\infty} F_{f_t}(x\sigma_N) f_{zl}(x, l)\mathrm{d}x \tag{10}$$

Based on a series of recent studies on strength distribution of brittle and quasibrittle materials [19,20,31], the material tensile strength f_t is considered to follow a grafted Gauss-Weibull distribution:

$$F_{f_t}(x) = \begin{cases} 1 - e^{-\langle x/s_0\rangle^m} \approx \langle x/s_0\rangle^m & (x \leq x_{\mathrm{gr}}) \quad (11a) \\ P_{\mathrm{gr}} + \dfrac{r_f}{\delta_G\sqrt{2\pi}}\displaystyle\int_{\sigma_{\mathrm{gr}}}^{x} e^{-(x'-\mu_G)^2/2\delta_G^2}\mathrm{d}x' & (x > x_{\mathrm{gr}}) \quad (11b) \end{cases}$$

where $\langle x\rangle = \max(x, 0)$, m is the Weibull modulus, s_0 is the Weibull scale parameter, μ_G and δ_G are the mean and standard deviation of the Gaussian distribution if extended to $-\infty$, P_{gr} is the grafting probability, which can be calculated as $P_{\mathrm{gr}} = (x_{\mathrm{gr}}/s_0)^m$, x_{gr} is the value of x at the grafting point, and r_f is the parameter. The grafted distribution contains six parameters, where any four of them can be taken as independent. The remaining two parameters can be solved by two constraints: (1) $F_{f_t}(\infty) = 1$, and (2) the pdf of the grafted distribution is continuous at the grafting point: $\mathrm{d}F_{f_t}(x)/\mathrm{d}x|_{x=x_{gr}^+} = \mathrm{d}F_{f_t}(x)/\mathrm{d}x|_{x=x_{gr}^-}$.

3 Large-Size Asymptotic Behavior

In this section we investigate the behavior of the present model at the large-size limit (i.e. $L \to \infty$). We first discuss the asymptotic distribution of segment number k based on the theory of renewal process [32–34]. We note that the probability distribution of the total length of a specimen that contains s number of segments, i.e. $F_L(L, s) = \Pr\left(\sum_{i=1}^{s} l_i \leq L\right)$. It is clear that s is a large number when $L \to \infty$. By the Central Limit Theorem, $F_L(L, s)$ would approach a Gaussian cdf:

$$F_L(L, s) \approx \Phi\left(\frac{L - s\mu_l}{\sqrt{s}\delta_l}\right) \tag{12}$$

where $\Phi(x)$ = standard Gaussian cdf, μ_l = the mean segment length, and δ_l = standard deviation of the segment length. Based on the Berry-Esseen theorem, the actual distribution $F_L(L, s)$ converges to the Gaussian cdf (Eq. (12)) with absolute error $\mathrm{O}(s^{-1/2})$.

Following Eq. (2), we can calculate the probability, $P(k, L)$, that a specimen of length L contains k number of V-notches as

$$P(k, L) = F_L(L, k) - F_L(L, k+1) \tag{13}$$

$$\approx \Phi\left(\frac{L - k\mu_l}{\sqrt{k}\delta_l}\right) - \Phi\left(\frac{L - (k+1)\mu_l}{\sqrt{(k+1)}\delta_l}\right) \tag{14}$$

Based on the Central Limit theory of renewal process [32,34], Eq. (14) leads to

$$P(k, L) = \frac{1}{\sqrt{2\pi L/\mu_l}\delta_l/\mu_l}\exp\left[-\frac{(k - L/\mu_l)^2}{2\delta_l^2 L/\mu_l^3}\right] \quad \text{when } L \to \infty \tag{15}$$

It is evident from Eq. (15) that, as L increases, the mean value of k approaches L/μ_l, and the standard deviation of k approaches $\omega_l\sqrt{L/\mu_l}$ (ω_l = coefficient of variation (CoV) of segment length l). Consequently, the CoV of k decreases as $L^{-1/2}$ for large L.

The simplest approach to derive the asymptotic strength distribution is to use the concept of stability postulate pioneered by Fisher and Tippett [12]. Here we divide the sidewall into p segments of equal length L_p, where p is a finite number. It follows that each segment length L_p also approaches infinity. Based on the weakest-link model, the strength distributions of the entire specimen and each segment can be related by

$$1 - P_f(\sigma_N) = [1 - P_{fp}(\sigma_N)]^p \tag{16}$$

where $P_{fp}(\sigma_N)$ = strength distribution of sidewall of length L_p. Since both the specimen length and segment length approach infinity, the strength distribution functions of the specimen and the segment must be of the same form and differ only by a linear transformation, i.e. $P_f(\sigma_N) = P_{fp}(k_1\sigma_N + k_2)$, where k_1, k_2 = parameters depending on p. Substituting this expression into Eq. (16), we have

$$P_{fp}(k_1\sigma_N + k_2) = 1 - [1 - P_{fp}(\sigma_N)]^p \tag{17}$$

Equation (17) is a functional equation representing the stability postulate. According to the theory of extreme value statistics [12,35,36], the functional form of $P_{fp}(\sigma_N)$ is determined by its left-tail behavior.

To determine the left-tail distribution, we note that the dimensionless stress is essentially bounded ($z \in [1, z_m]$). Equation (8) indicates that, at small stresses, the reliability of each segment containing a V-notch can be expressed by

$$R_e(\sigma_N, l) = 1 - \left[\frac{1}{f(l)}\int_0^{z_m} x^m f_{zl}(x, l)\mathrm{d}x\right]\left(\frac{\sigma_N}{s_0}\right)^m \tag{18}$$

Substituting Eq. (18) into Eq. (3) yields

$$R(\sigma_N, L_p, k) = \int_0^{L_p} \int_0^{L_p - l_1} \cdots \int_0^{L_p - l_1 \cdots - l_{k-1}} \left\{ \prod_{i=1}^{k} f(l_i)[1 - \psi(l_i)(\sigma_N/s_0)^m] \right\} F_c(L_p - l_1 \cdots - l_k) \mathrm{d}l_k \mathrm{d}l_{k-1} \cdots \mathrm{d}l_1 \tag{19}$$

where $\psi(l_i) = [\int_0^{z_m} x^m f_{zl}(x, l_i)\mathrm{d}x]/f(l_i)$. By expanding the term $\prod_{i=1}^{k} f(l_i)[1 - \psi(l_i)(\sigma_N/s_0)^m]$ and retaining the leading terms up to σ_N^m, we

$$\prod_{i=1}^{k} f(l_i)[1 - \psi(l_i)(\sigma_N/s_0)^m] \approx \prod_{i=1}^{k} f(l_i) - \left(\prod_{i=1}^{k} f(l_i) \right) \left(\sum_{i=1}^{k} \psi(l_i) \right) (\sigma_N/s_0)^m \quad (\text{as } \sigma_N \to 0) \tag{20}$$

Therefore, Eq. (19) can be rewritten as

$$R(\sigma_N, L_p, k) = P(k, L_p) - C(k, L_p) \left(\frac{\sigma_N}{s_0} \right)^m \tag{21}$$

where:

$$P(k, L_p) = \int_0^{L_p} \int_0^{L_p - l_1} \cdots \int_0^{L_p - l_1 \cdots - l_{k-1}} \prod_{i=1}^{k} f(l_i) F_c(L_p - l_1 \cdots - l_k) \mathrm{d}l_k \mathrm{d}l_{k-1} \cdots \mathrm{d}l_1 \tag{22}$$

$$C(k, L_p) = \int_0^{L_p} \int_0^{L_p - l_1} \cdots \int_0^{L_p - l_1 \cdots - l_{k-1}} \left(\prod_{i=1}^{k} f(l_i) \right) \left(\sum_{i=1}^{k} \psi(l_i) \right) F_c(L_p - l_1 \cdots - l_k) \mathrm{d}l_k \mathrm{d}l_{k-1} \cdots \mathrm{d}l_1 \tag{23}$$

We note that $P(k, L_p)$ = probability that a specimen of length L_p contains k number of V-notches. Clearly, we have $\sum_{k=1}^{\infty} P(k, L_p) = 1$, and the reliability of the entire specimen (Eq. (1)) becomes

$$R(\sigma_N, L_p) = \left\{ 1 - \sum_{k=1}^{\infty} C(k, L_p) \left(\frac{\sigma_N}{s_0} \right)^m \right\}^2 \quad (\text{as } \sigma_N \to 0) \tag{24}$$

$$\text{or:} \quad P_f(\sigma_N, L_p) \approx C_0(L_p) \left(\frac{\sigma_N}{s_0} \right)^m \quad (\text{as } \sigma_N \to 0) \tag{25}$$

where $C_0(L_p) = 2 \sum_{k=1}^{\infty} C(k, L_p)$.

Equation (25) indicates that the failure probability of a sidewall has a power-law left tail. Based on the theory of extreme statistics, the only possible distribution function that satisfies the stability postulate (Eq. (17)) is the Weibull distribution, i.e.

$$P_f(\sigma_N) = 1 - \exp[-(\sigma_N/S)^m] \tag{26}$$

where S = a parameter proportional to $L^{-1/m}$. It should be emphasized that, as indicated by Eq. (18), the strength distribution of a single segment has a power-law tail, which arises from the tail distribution of the local material strength. The power-law tail behavior of the strength of a single segment dictates the asymptotic form of the Weibullian strength distribution of the entire specimen at the large-size limit.

4 Comparison with Experimental Data

We now compare the proposed model with the measured strength distributions of uniaxial tensile poly-Si MEMS specimens. Two sets of experimental data are considered. The first data set consists of strength distributions of specimens of two gauge lengths ($L = 20$ and 70 μm) [9,37]. The nominal width of specimens of both lengths is 2 μm. The 70 μm-long specimens were tested using an on-chip tester, which involved a Chevron thermal actuator with a prehensile grip mechanism. The 20 μm-long specimens were tested using a slack-chain tester, where a number of specimens were placed in a chain and loaded by a custom-built probe station. The second data set consists of strength distributions of specimens of gauge lengths of 7 and 70 μm, which were tested using an on-chip tester [17]. For both data sets, the specimens were produced by Sandia's SUMMiT V poly-Si microfabrication process [38]. Therefore, it is reasonable to assume that all specimens share the similar random sidewall geometry.

To use the present model, we first determine the dimensionless stress z as a deterministic function of segment length l, notch depth a, and notch angle θ through a series of finite element simulations. It is noted that the specimen width is significantly larger than the notch depth, and meanwhile the spacing of the adjacent V-notches is considerably larger than the notch depth as well as the width of FPZ. Therefore, it is reasonable to assume that all the V-notches are non-interacting for the calculation of the elastic stress field of the near-tip region. In the finite element simulation, we consider a segment of uniaxial tensile specimen containing a V-notch at the middle under a unit far-field stress ($\sigma_N = 1$), as shown in Fig. 2. The material is modeled as isotropic with Young modulus $E = 156$ GPa and Poisson ratio $\mu = 0.22$ [8]. To calculate the dimensionless stress, we consider the averaging zone size r_c to be 5 nm, which is on the order of the FPZ size of poly-Si [8,16,38].

The random geometry of the sidewall can be characterized by three random variables (Fig. 2): (1) the notch angle θ, (2) the notch depth a, and (3) the representative notch spacing c. The existing experimental analysis of the sidewall geometry provides the approximate range of these geometrical variables, but not the full distribution functions. For the sake of simplicity, we assume θ and c to follow bounded uniform distributions. For the notch depth, we assume a Type III extreme value distribution with an upper bound equals 62 nm [16,21]. The pdfs of θ, a, and c are given by

$$f_\theta(\theta) = \frac{1}{120} \quad (20^\circ \le \theta \le 140^\circ) \tag{27}$$

$$f_a(a) = 0.232 \left(\frac{62 - a}{28} \right)^{5.5} \exp\left[-\left(\frac{62 - a}{28} \right)^{6.5} \right] \quad (0 \le a \le 62\,\text{nm}) \tag{28}$$

$$f_c(c) = \frac{1}{600} \quad (100\,\text{nm} \le c \le 700\,\text{nm}) \tag{29}$$

where f_θ, f_a and f_c are the pdfs of θ, a, and c, respectively. Note that Eq. (28) permits negative values of a, which is physically inadmissible. However, it is unlikely that a negative value would be sampled since $\Pr(a \le 0) = 6.7 \times 10^{-77}$.

Based on the notch geometry, the segment length can be expressed by $l = c + 2a\tan(\theta/2)$. The probability distribution of l can be calculated analytically as

$$f(l) = \int_0^l f_c(l-y) f_q(y)\mathrm{d}y \tag{30}$$

$$\text{where:} \quad f_q(x) = \int_0^\infty \frac{4}{4y + y^3} f_\theta\left(2\tan^{-1}(y/2)\right) f_a(x/y)\mathrm{d}y \tag{31}$$

It should be pointed out that the range of possible values of a, θ, and c implies a finite minimum value of the segment length, below which we have $f(l) = 0$. Figure 3 shows the pdf of segment length based on Eq. (30), which matches well the result of direct Monte Carlo simulations.

To obtain the joint pdf of dimensionless stress and segment length, a total of 10^7 groups of a, θ and l are sampled from the distribution functions described by Eqs. (27), (28), and (30). For each group of a, θ and l, we calculate the corresponding value of z by interpolating the simulated function $z(a, \theta, l)$. Based on these groups of z and l values, we obtain the joint pdf $f_z(z, l)$, which is presented in Fig. 4.

After determining the pdf of segment length and the joint pdf $f_{zl}(z, l)$, we use the present model to fit the aforementioned measured strength distributions. What needs to be calibrated is the cdf of local material strength, $F_{f_l}(x)$, i.e. the Weibull modulus m, the Weibull scale parameter s_0, the mean value μ_G and the standard deviation δ_G of the Gaussian core. Figures 5 and 6 show the optimum fitting of the measured strength distributions. The corresponding fitted parameters of the material strength distribution listed are as follows: data set 1: $\mu_G = 16.5$ GPa, $\delta_G = 0.99$ GPa, $m = 64$, $s_0 = 15.4$ GPa; data set 2: $\mu_G = 17.2$ GPa, $\delta_G = 1.03$ GPa, $m = 64$, $s_0 = 16.1$ GPa.

Figures 5 and 6 show that the present model can match well the measured strength distributions of specimens of two different gauge lengths. Clearly the measured distributions cannot be fitted by the two-parameter Weibull distribution, which is represented by a straight line in the Weibull scale. In order to improve the fitting of experimental data, recent studies suggested the three-parameter Weibull distribution [17], which introduces a strength threshold to the two-parameter Weibull model. However, the functional form of the three-parameter Weibull distribution still rests on the extreme value statistics. For specimens considered here, the extreme value statistics would be valid if there are a large number (at least $>10^5$) of V-notches along the sidewall. However, this is not the case for specimens of a gauge length on the order of 10 – 100 μm, which contain about several hundred V-notches. The agreement between the present model and the experimental data

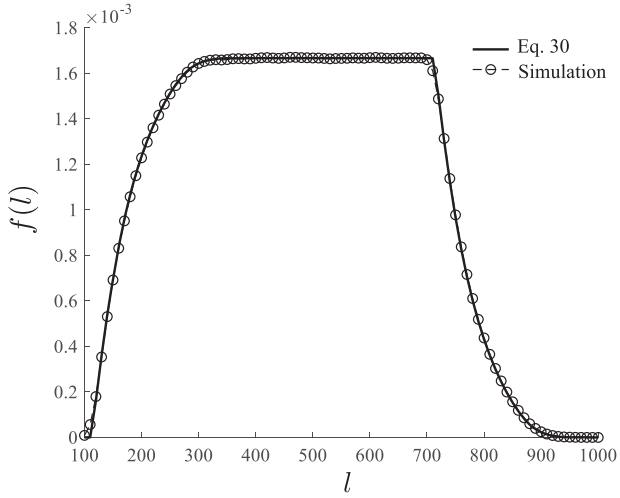

Fig. 3 Calculated pdf of segment length

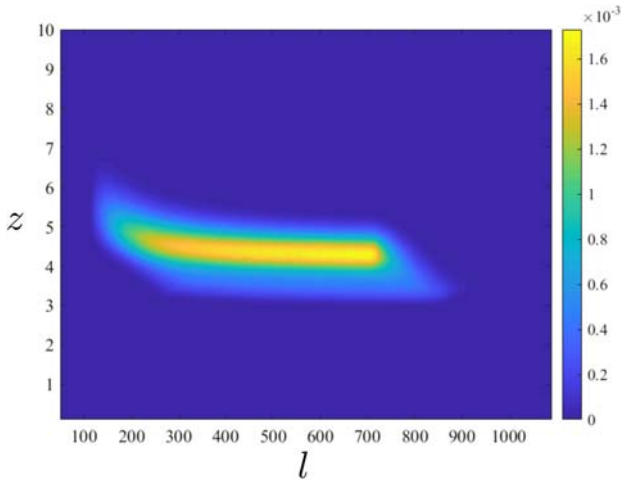

Fig. 4 Joint pdf $f_{zl}(z, l)$ of the dimensionless stress field

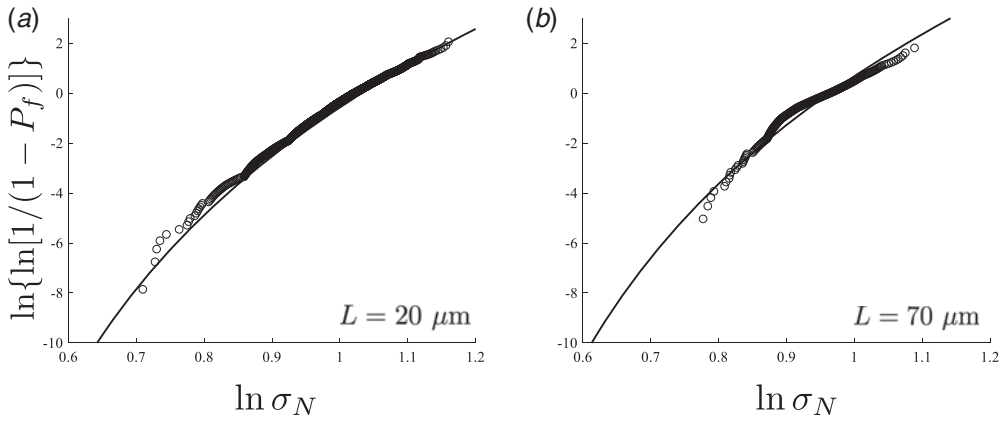

Fig. 5 Optimum fits of the measured strength histograms (data set 1) by the present model

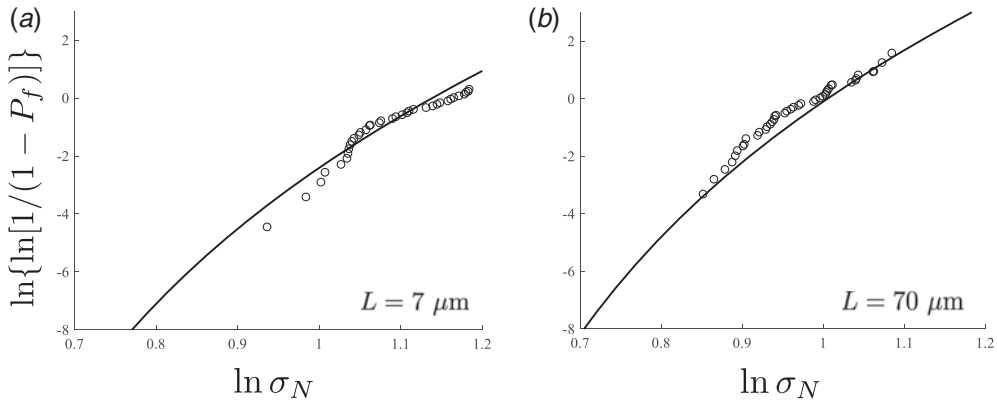

Fig. 6 Optimum fits of the measured strength histograms (data set 2) by the present model

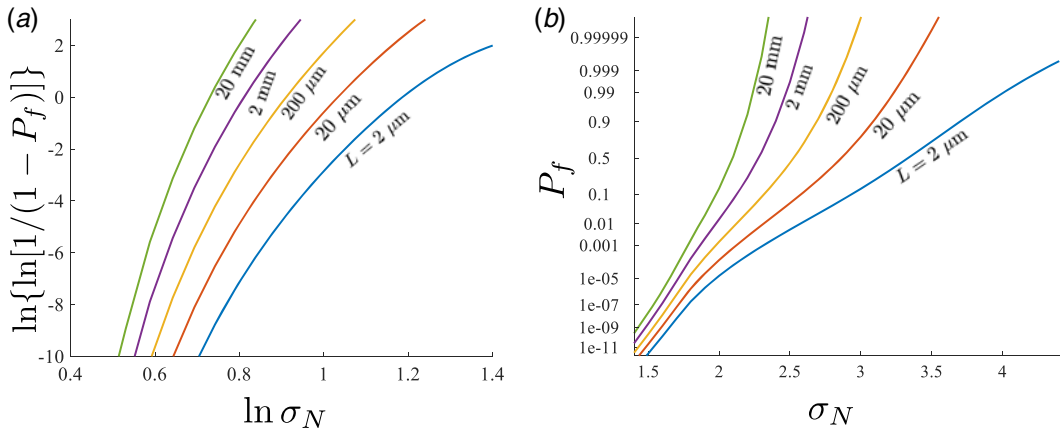

Fig. 7 Predicted strength distributions of MEMS specimens of different lengths presented in (*a*) Weibull distribution paper and (*b*) Gaussian distribution paper

indicates that the strength threshold is unnecessary. The underlying reason for the deviation of the measured strength distribution from the two-parameter Weibull model is the finite random number of V-notches along the sidewall.

5 Size Effect Analysis

As shown in Figs. 5 and 6, one salient feature of the strength distribution of MEMS specimens is its pronounced dependence on the specimen size. Capturing this size effect has become an essential aspect of model validation. For the conventional Weibull models (e.g. two and three-parameter Weibull distributions), which are anchored by the weakest-link statistics, the specimen size only influences the Weibull scale parameter, and consequently the size effect on the strength distribution manifests as a horizontal shift of the strength cdf in the Weibull scale [20]. Based on Figs. 5 and 6, it is evident that, even with rather a limited size range, the size effect on the strength distribution cannot be captured by a simple horizontal shift in the Weibull scale. This suggests that the classical Weibull models could not be used for design extrapolation for MEMS devices of different sizes.

The present model naturally yields an intricate size effect on the strength distribution, as indicated by Eq. (3). Figure 7 plots in both Weibull and Gaussian distribution papers the predicted strength cdfs of specimens of different lengths by using the model parameters calibrated based on data set 1. It is seen that, for small-size specimens, the strength cdf deviates significantly from the two-parameter Weibull distribution, and in fact it can be better approximated by a Gaussian distribution except for the left tail portion. As the specimen size increases, the strength cdf starts to approach the Weibull distribution. As indicated by the foregoing analysis of large-size asymptotic behavior, the strength distribution at the large-size limit must follow the two-parameter Weibull distribution. Therefore, the specimen size influences not only the mean and standard deviation of the strength distribution, but more fundamentally the functional form of the distribution.

It should be mentioned that previous studies also proposed to use three-parameter Weibull distributions with size-dependent Weibull modulus, scale parameter, and strength threshold [17]. Such models can fit the measured strength distribution of MEMS specimens of different sizes. However, in addition to the aforementioned questionable assumption of the Weibull statistical model, there is a lack of physical relationship between these model parameters and the specimen size, and consequently the prediction capability of such models is rather limited.

Figure 8 plots the probability distributions of the number of V-notches for different specimen sizes with comparison to Eq. (15). It is observed that, as the specimen length increases, the pdf of k approaches Eq. (15), which justifies that foregoing analysis of the large-size asymptotic behavior. In fact, Eq. (15) could provide a reasonable approximation of the distribution of k even for intermediate specimen size $L > 20\ \mu$m (i.e. $\bar{k} \geq 423$). It is also found that, for all specimen lengths, the expected value of k can be reasonably approximated as $\bar{k} = L/\mu_l$.

One direct consequence of the aforementioned size dependence of the strength cdf is the size effect on the mean structural strength, as shown in Fig. 9. The size effect shown here arises from the weakest-link failure statistics, which is often referred to as the statistical size effect. It is noted that, in principle, there exists another size effect associated with the fracture of V-notch [30], which is related to the constancy of fracture energy. This size effect, which is of deterministic nature, is defined as the energetic

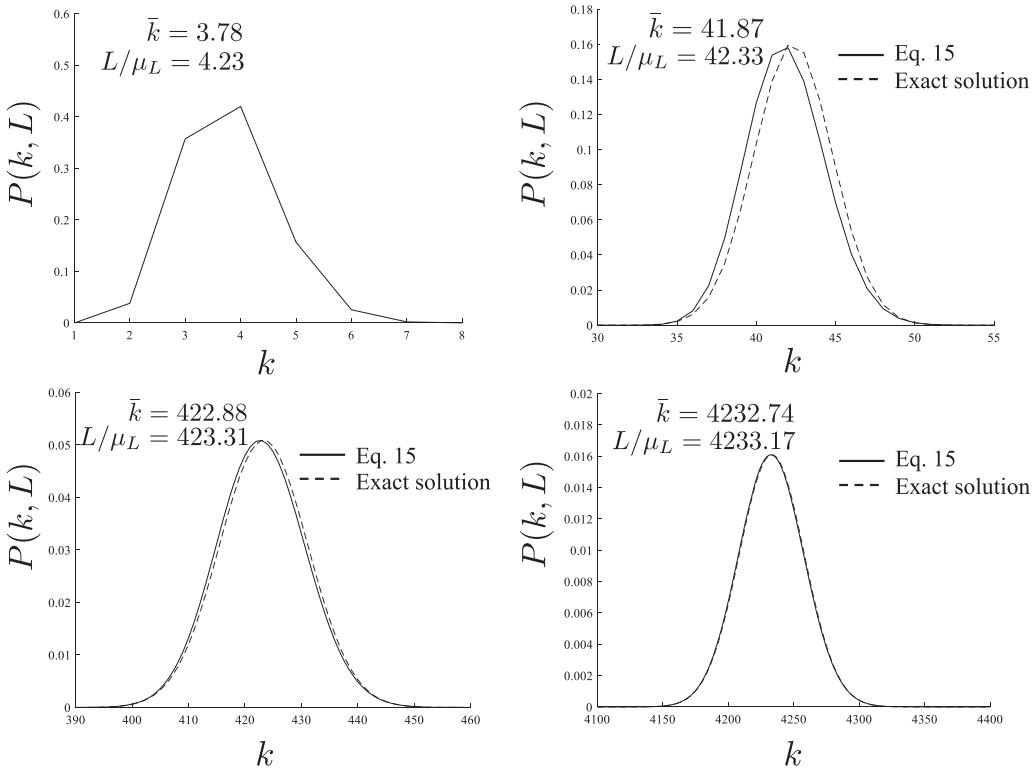

Fig. 8 Probability distributions of the number of V-nocthes for different specimen lengths

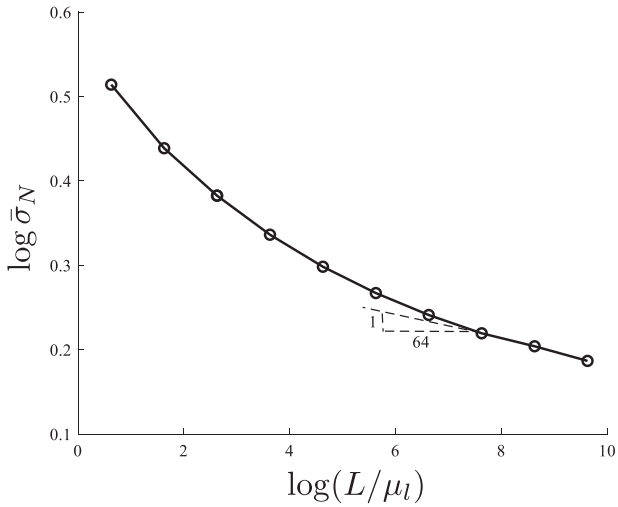

Fig. 9 Size effect on the mean structural strength

size effect. However, the energetic size effect is not manifested here since the notch size and the specimen width are not scaled.

The calculated size effect shown in Fig. 9 is qualitatively similar to the Type 1 size effect curve for quasibrittle structures [20,40,41], which can be approximated by

$$\bar{\sigma}_N(L) = \mu_G\left[\frac{\eta_1\mu_l}{L} + \left(\frac{\eta_2\mu_l}{L}\right)^{r/q}\right]^{1/r} \tag{32}$$

where η_1, η_2, r, q = constants. At the large-size limit, the strength distribution converges to the Weibull distribution, and based on Eq. (26) the mean strength should scale with the specimen length as $\bar{\sigma}_N \propto L^{-1/m}$. On the other hand, the large-size asymptote of Eq. (32) follows $\bar{\sigma}_N \approx \mu_G(\eta_2\mu_l/L)^{1/q}$. Therefore, we may conclude that $q = m$. Meanwhile, at the large-size limit, what matters for the failure statistics is the Weibull tail of the material strength cdf. $\mu_G\eta_2^{1/m}$ must be related to the Weibull scale parameter s_0 of Eq. (32), i.e. $\mu_G\eta_2^{1/m} = f_1(s_0)$.

At the small-size limit (i.e. $L \to l_m$, $l_m \approx 1.5\,\mu$m = the smallest size of the specimen for the random sidewall geometry considered here), Eq. (32) converges to $\bar{\sigma}_N \approx \mu_G(\eta_1\mu_l/l_m)^{1/r}$. In this case, only the Gaussian part of the material strength cdf is relevant for the failure statistics. We may consider the mean strength and the slope of the mean size effect curve, both of which are governed by the mean and standard deviation of the Gaussian core of Eq. (11), i.e. $\bar{\sigma}_N(l_m) = f_2(\mu_G, \delta_G)$, and $\mathrm{d}\bar{\sigma}_N/\mathrm{d}L|_{L=l_m} = f_3(\mu_G, \delta_G)$. Combining the aforementioned large and small-size asymptotic conditions, we can relate the properties of the mean size effect curve to the strength distribution of local material strength. This is an attractive alternative to the histogram testing method. This size effect analysis has recently been validated for some quasibrittle materials, e.g. cold asphalt mixtures, based on the conventional weakest-link model without considering the random stress field [42].

6 Simplified Calculation Approach

It is clear that the main computational cost of the present model arises from the evaluation of the multiple integrations in Eq. (3), which is handled by the recursive equations (Eqs. (4) and (6)). However, for long specimens, the computation becomes tedious. It would be desirable to develop a simplified calculation method.

The direct way to avoid evaluating the multiple integration of Eq. (3) is to approximate the reliability of each segment by a function that is independent of segment length. One plausible choice is to use the expectation of the segment reliability, i.e.:

$$\bar{R}_e(\sigma_N) = \int_0^\infty R_e(\sigma_N, l)f(l)\mathrm{d}l \tag{33}$$

$$= 1 - \int_0^\infty F_{f_l}(x\sigma_N) f_z(x)\mathrm{d}x \tag{34}$$

where $f_z(x) = \int_0^\infty f_{zl}(x, l)\mathrm{d}l =$ marginal distribution of the dimensionless stress. The error due to this approximation may be evaluated by

$$\Delta_1(\sigma_N) = \int_0^\infty f(l) \frac{|R_e(\sigma_N, l) - \bar{R}_e(\sigma_N)|}{R_e(\sigma_N, l)} \mathrm{d}l \tag{35}$$

As will be shown later, $\Delta_1(\sigma_N)$ is negligibly small for specimens considered in this study.

Based on the aforementioned approximation (Eq. (33)), the reliability of a single sidewall of length L can be expressed by

$$R(\sigma_N, L) \approx \sum_{k=1}^{\infty} P(k, L)\left[\bar{R}_e(\sigma_N)\right]^k \tag{36}$$

where $P(k, L)$ is defined in Eq. (22). By taking the logarithm of Eq. (36), we have

$$\ln R(\sigma_N, L) = \ln\{\mathbb{E}_k[Y(\sigma_N, k)]\} \tag{37}$$

where $Y(\sigma_N, k) = \left[\bar{R}_e(\sigma_N)\right]^k$, and $\mathbb{E}_k(\cdot) =$ expectation with respect to k. The logarithm of the expectation of $Y(\sigma_N, k)$ can be further approximated by $\ln\{\mathbb{E}_k[Y(\sigma_N, k)]\} \approx \mathbb{E}_k\{\ln Y(\sigma_N, k)\} + \frac{1}{2}\omega_Y^2(\sigma_N, L)$, where $\omega_Y(\sigma_N, L) =$ CoV of $Y(\sigma_N, k)$. It will be shown later that, for specimens considered in this study, we may neglect the term $\frac{1}{2}\omega_Y^2(\sigma_N, L)$ and consider

$$\ln\{\mathbb{E}_k[Y(\sigma_N, k)]\} \approx \mathbb{E}_k\{\ln Y(\sigma_N, k)\} \tag{38}$$

The resulting error, which depends on both σ_N and specimen length L, can be calculated as

$$\Delta_2(\sigma_N, L) = \left|1 - \frac{\mathbb{E}_k\{\ln Y(\sigma_N, k)\}}{\ln\{\mathbb{E}_k[Y(\sigma_N, k)]\}}\right| \tag{39}$$

By combining Eqs. (37) and (38), we have

$$\ln R(\sigma_N, L) \approx \mathbb{E}_k\{\ln Y(\sigma_N, k)\} \tag{40}$$

$$= \sum_{k=1}^{\infty} P(k, L) k \bar{R}_e(\sigma_N) = \bar{k}(L)\bar{R}_e(\sigma_N) \tag{41}$$

where $\bar{k}(L) =$ mean value of k for a given sidewall length L. Equation (41) suggests that the overall failure probability of the specimen can be approximately calculated as

$$P_f(\sigma_N, L) = 1 - \left[\bar{R}_e(\sigma_N)\right]^{2\bar{k}} \tag{42}$$

It is evident that Eq. (42) can be considered as an equivalent weakest-link model, which uses the expected number of V-notches and the expectation of segment reliability. As shown in Fig. 8, we may further approximate $\bar{k}$ as L/μ_l. The computation of $\bar{R}_e(\sigma_N)$ requires the detailed information of the statistics of segment length.

As a demonstration, we apply this simplified calculation method to recalculate the strength distribution of specimens with its parameters calibrated by data set 1. Here we consider four different specimens sizes $L = 1.5$, 20, 200, and 2000 μm. Figure 10 shows that the strength distributions of these specimens calculated by the full model (Eqs. (1) and (3)) and the simplified model (Eq. (42)). It is found that these two models agree with each other very well for specimens of $L = 20$, 200, 2000 μm, which covers the size range of typical MEMS specimens. For the smallest specimen, two models deviate from each other in the high stress regime ($\sigma_N \geq$ 3.7 GPa).

To explain the aforementioned observation, we examine the two approximations introduced in the simplified method (i.e. Eqs. (33) and (38)). Figure 11 shows the expected relative error, $\Delta_1(\sigma_N)$, for the relevant range of nominal stress. It is seen that $\Delta_1(\sigma_N)$ increases with the nominal stress σ_N. The error grows beyond 1%

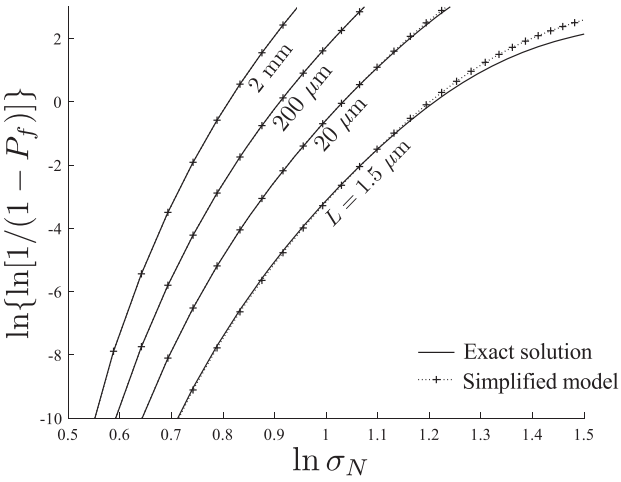

Fig. 10 Comparison of the strength distributions of MEMS specimens predicted by the renewal weakest-link model and the simplified model

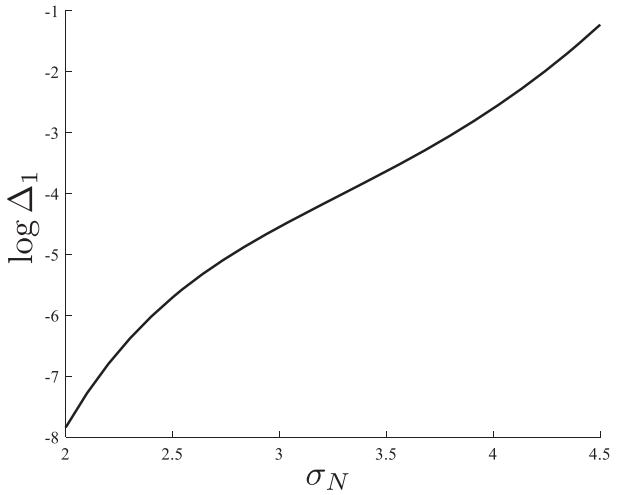

Fig. 11 Plot of relative error $\Delta_1(\sigma_N)$ defined in Eq. (35)

as $\sigma_N > 4.2$ GPa. Meanwhile, we also plot the relative error $\Delta_2(\sigma_N, L)$ due to Eq. (38) for different specimen lengths (Fig. 12). It is seen that for specimens of $L = 20$, 200, 2000 μm, the relative error is below 10^{-3}. For specimen of $L = 1.5$ μm, the error is larger than 1% when $\sigma_N > 4$ GPa.

The foregoing analysis of the two approximations indicates that the error of the simplified method would become significant only in the high stress regime. Due to the presence of the size effect, the relevant stress level for estimating the failure probability of typical MEMS specimens ($L \geq 5$ μm) does not fall into this high stress regime. This indicates that the proposed simplified method can be applied to most specimens, as shown in Fig. 10. As compared to Eqs. (1) and (3), the simplified model (Eq. (42)) is far more efficient since it does not require the calculation of multiple integrations for all different possible segment lengths and different σ_N values. This makes the computation of the present renewal weakest-link model essentially the same as the conventional weakest-link model, such as [16].

7 Conclusions

A renewal weakest-link model is developed for strength statistics of uniaxial tensile poly-Si MEMS specimens. The model explicitly considers both the random spacing and geometry of the sidewall

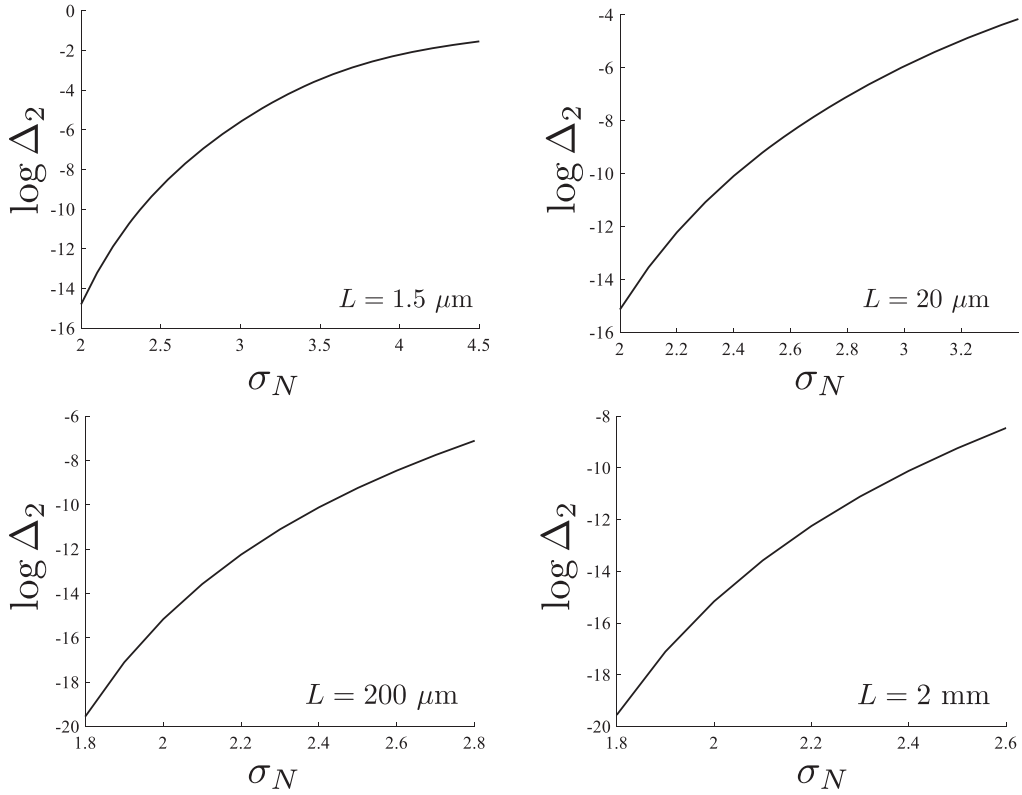

Fig. 12 Plot of relative error $\Delta_2(\sigma_N, L)$ defined in Eq. (39)

grooves. It is shown that, at the large-size limit, the model predicts a Weibullian strength distribution, which is consistent with the theory of extreme value statistics. The model agrees well with the measured strength distributions of MEMS specimens of different lengths.

The salient feature of the model is that it predicts an intricate size effect on the strength distribution of MEMS specimens, which gives rise to a mean size effect curve. Within the present model framework, the asymptotic properties of the mean size effect curve can be related to the statistical properties of the local material strength. The relationship implies that the failure statistics of the specimen can be determined from the mean size effect curve, which is much more efficient than the conventional histogram testing method.

It is shown that the present renewal weakest-link model can be approximated by an equivalent weakest-link model. The model uses only the average number of surface grooves and the expectation of the reliability function of each groove. This simplification provides an efficient means for determining the strength distribution of MEMS specimens.

Acknowledgment

Financial support under NSF Grant CMMI-1361868 to the University of Minnesota and the University of Houston is gratefully acknowledged.

References

[1] Boyce, B. L., Ballarini, R., and Chasiotis, I., 2008, "An Argument for Proof Testing Brittle Microsystems in High-Reliability Applications," J. Micromech. Microeng., **18**(11), p. 117001.
[2] Jiang, L., and Spearing, S. M., 2012, "A Reassessment of Materials Issues in Microelectromechanical Systems (MEMS)," J. Indian Inst. Sci., **87**(3), p. 363.
[3] Ballarini, R., Kahn, H., Heuer, A. H., de Boer, M. P., and Dugger, M. T., 2007, "MEMS Structures for On-Chip Testing of Mechanical and Surface Properties of Thin Films," Comprehensive Structural Integrity, I. Milne, R. Ritchie, and B. Karihaloo, eds., Elsevier, New York.
[4] Kahn, H., Chen, L., Ballarini, R., and Heuer, A. H., 2006, "Mechanical Fatigue of Polysilicon: Effects of Mean Stress and Stress Amplitude," Acta Mater., **54**(3), pp. 667–678.
[5] Ballarini, R., 1998, "The Role of Mechanics in Microelectromechanical Systems (MEMS) Technology," Air Force Research Laboratory, Dayton, OH, Technical Report No. AFRL-ML-WP-TR-1998-4209.
[6] Espinosa, H. D., Peng, B., Moldovan, N., Friedmann, T. A., Xiao, X., Mancini, D. C., Auciello, O., Carlisle, J., and Zorman, C. A., 2005, "A Comparison of Mechanical Properties of Three MEMS Materials-Silicon Carbide, Ultrananocrystalline Diamond, and Hydrogen-Free Tetrahedral Amorphous Carbon (Ta-C)," 11th International Conference on Fracture, Vol. 5, A. Carpinteri, ed., Turin, Italy, Mar. 20–25, pp. 3806–3811.
[7] Fitzgerald, A. M., Pierce, D. M., Huigens, B. M., and White, C. D., 2009, "A General Methodology to Predict the Reliability of Single-Crystal Silicon MEMS Devices," J. Microelectromech. Syst., **18**(4), pp. 962–970.
[8] Reedy, E. D., Jr., 2011, "Singular Stress Fields at the Intersection of a Grain Boundary and a Stress-Free Edge in a Columnar Polycrystal," ASME J. Appl. Mech., **78**, p. 014502.
[9] Reedy, E. D., Jr., Boyce, B. L., Foulk, J. W., III, Field, R. V., Jr., de Boer, M. P., and Hazra, S. S., 2011, "Predicting Fracture in Micrometer-Scale Polycrystalline Silicon MEMS Structures," J. Microelectromech. Syst., **20**(4), pp. 922–932.
[10] Weibull, W., 1939, "The Phenomenon of Rupture in Solids," Proc. Royal Sweden Inst. Engrg. Res., **153**, pp. 1–55.
[11] Weibull, W., 1951, "A Statistical Distribution Function of Wide Applicability," ASME J. Appl. Mech., **153**(18), pp. 293–297.
[12] Fisher, R. A., and Tippett, L. H. C., 1928, "Limiting Form of the Frequency Distribution the Largest and Smallest Number of a Sample," Proc. Cambridge Philos. Soc., **24**, pp. 180–190.
[13] Gumbel, E. J., 1958, *Statistics of Extremes*, Columbia University Press, New York.
[14] Espinosa, H. D., Peng, B., Moldovan, N., Friedmann, T. A., Xiao, X., Mancini, D. C., Auciello, O., Carlisle, J., and Zorman, C. A., 2005, "A Comparison of Mechanical Properties of Three MEMS Materials–Silicon Carbide, Ultrananocrystalline Diamond, and Hydrogen-Free Tetrahedral Amorphous Carbon (Ta-C)," 11th International Conference on Fracture, Turin, Italy, Mar. 20–25, A. Carpinteri, ed., Vol. 5, pp. 3806–3811.
[15] Boyce, B. L., Grazier, J. M., Buchheit, T. E., and Shaw, M. J., 2007, "Strength Distributions in Polycrystalline Silicon MEMS," J. Microelectromech. Syst., **16**(2), pp. 179–190.
[16] Le, J.-L., Ballarini, R., and Zhu, Z., 2015, "Modeling of Probabilistic Failure of Polycrystalline Silicon MEMS Structures," J. Amer. Cer. Soc., **98**(6), pp. 1685–1697.
[17] Saleh, M. E., Beuth, J. L., and de Boer, M. P., 2014, "Validated Prediction of the Strength Size Effect in Polycrystalline Silicon Using the Three-Parameter Weibull Function," J. Amer. Cer. Soc., **97**(12), pp. 3982–3990.

[18] Pang, S.-D., Bažant, Z. P., and Le, J.-L., 2008, "Statistics of Strength of Ceramics: Finite Weakest Link Model and Necessity of Zero Threshold," Int. J. Frac., **154**, pp. 131–145.
[19] Le, J.-L., Bažant, Z. P., and Bazant, M. Z., 2011, "Unified Nano-Mechanics Based Probabilistic Theory of Quasibrittle and Brittle Structures: I. Strength, Crack Growth, Lifetime and Scaling," J. Mech. Phys. Solids, **59**, pp. 1291–1321.
[20] Bažant, Z. P., and Le, J.-L., 2017, *Probabilistic Mechanics of Quasibrittle Structures: Strength, Lifetime, and Size Effect*, Cambridge University Press, Cambridge, UK.
[21] Xu, Z., and Le, J.-L., 2017, "A First Passage Model for Probabilistic Failure of Polycrystalline Silicon MEMS Structures," J. Mech. Phys. Solids, **99**, pp. 225–241.
[22] Bažant, Z. P., and Ohtsubo, H., 1977, "Stability Conditions for Propagation of a System of Cracks in a Brittle Solid," Mech. Res. Comm., **4**(5), pp. 353–366.
[23] Nemat-Nasser, S., Keer, L. M., and Parihar, K. S., 1978, "Unstable Growth of Thermally Induced Interacting Cracks in Brittle Solids," Int. J. Solids Struct., **14**(6), pp. 409–430.
[24] Bažant, Z. P., Salviato, M., Chau, V. T., Viswanathan, H., and Zubelewicz, A., 2014, "Why Fracking Works," J. Appl. Mech. ASME, **81**, p. 101010 (10 pages).
[25] Carpinteri, A., 1987, "Stress-Singularity and Generalized Fracture Toughness at the Vertex of Reentrant Corners," Engrg. Frac. Mech., **26**, pp. 143–155.
[26] Seweryn, A., 1994, "Brittle Fracture Criterion for Structures with Sharp Notches," Engrg. Fract. Mech., **47**, pp. 673–681.
[27] Dunn, M. L., Suwito, W., and Cunningham, S. J., 1997, "Fracture Initiation at Sharp Notches: Correlation Using Critical Stress Intensities," Int. J. Solids Struct., **34**(29), pp. 3873–3883.
[28] Leguillon, D., 2002, "Strength or Toughness? A Criterion for Crack Onset at a Notch," Eur. J. Mech., A/Solids, **21**, pp. 61–72.
[29] Gomez, F. J., and Elices, M., 2003, "A Fracture Criterion for Sharp V-Notched Samples," Int. J. Frac., **123**(3–4), pp. 163–175.
[30] Le, J.-L., Pieuchot, M., and Ballarini, R., 2014, "Effect of Stress Singularity Magnitude on Scaling of Strength of Quasibrittle Structures," J. Engrg. Mech. ASCE, **140**(5), p. 04014011.
[31] Bažant, Z. P., Le, J.-L., and Bazant, M. Z., 2009, "Scaling of Strength and Lifetime Distributions of Quasibrittle Structures Based on Atomistic Fracture Mechanics," Proc. Nat'l. Acad. Sci., USA, **106**, pp. 11484–11489.
[32] Cox, D. R., 1967, *Renewal Theory*, Vol. 1, Methuen & Co, London.
[33] Ang, A. H. S., and Tang, W. H., 1984, *Probability Concepts in Engineering Planning and Design. Vol II. Decision, Risk and Reliability*, J. Wiley, New York.
[34] Kulkarni, V. G., 2016, *Modeling and Analysis of Stochastic Systems*, 2 ed., Chapman and Hall/CRC, Boca Raton.
[35] Kotz, S., and Nadarajah, S., 2000, *Extreme Value Distributions: Theory and Applications*, Imperial College Press, London.
[36] Vanmarcke, E., 2010, *Random Fields Analysis and Synthesis*, World Scientific Publishers, Singapore.
[37] Hazra, S. S., Baker, M. S., Beuth, J. L., and de Boer, M. P., 2009, "Demonstration of an In-Situ On-Chip Tester," J. Micromech. Microeng., **19**, p. 082001 (5 pp.).
[38] Sniegowski, J. J., and de Boer, M. P., 2000, "IC-Compatible Polysilicon Surface Micromachining," Annu. Rev. Mater. Sci., **30**, pp. 299–333.
[39] Yasutake, K., Iwata, M., Yoshii, K., Umeno, M., and Kawabe, H., 1986, "Crack Healing and Fracture Strength of Silicon Crystals," J. Mater. Sci., **21**(6), pp. 2185–2192.
[40] Bažant, Z. P., 2004, "Scaling Theory of Quaisbrittle Structural Failure," Proc. Nat'l. Acad. Sci., USA, **101**(37), pp. 13400–13407.
[41] Bažant, Z. P., 2005, *Scaling of Structural Strength*, Elsevier, London.
[42] Le, J.-L., Cannone Falchetto, A., and Marasteanu, M. O., 2013, "Determination of strength distribution of quasibrittle structures from mean size effect analysis," Mech. Mater., **66**, pp. 79–87.